

BaRh₂Si₉ – a new clathrate with a rhodium–silicon framework

Cite this: *Dalton Trans.*, 2014, **43**, 2140

Walter Jung,^{*a,b} Alim Ormeci,^a Walter Schnelle,^a Hong Duong Nguyen,^a Michael Baitinger^a and Yuri Grin^{*a}

The semiconducting compound BaRh₂Si₉ is a new kind of intermetallic clathrate. It was obtained by reacting BaSi, Rh and Si at 950 °C. The crystal structure (space group *C2/c*; Pearson symbol *mC48*, *a* = 6.2221(5) Å, *b* = 21.399(2) Å, *c* = 6.2272(5) Å, β = 90.306(7)°) displays a covalently bonded Rh–Si framework, in which four-connected Si atoms partly show unusually small bond angles. The Ba atoms are encapsulated in large polyhedral cages formed by 18 Si and 4 Rh atoms. The compound is a diamagnetic p-type semiconductor, which is in agreement with band structure calculations resulting in a band gap of 0.12 eV. Quantum chemical calculations reveal positively charged Ba atoms (Ba^{+1.3}) and negatively charged Rh atoms (Rh⁻¹). Si atoms with neighboring Rh atoms are positively charged, while those connected only with Si atoms are negatively charged.

Received 4th October 2013,
Accepted 4th November 2013

DOI: 10.1039/c3dt52775a

www.rsc.org/dalton

1. Introduction

Semiconducting framework compounds based on silicon networks always attract interest in physics and materials science for their transport properties. By modifying both the crystal structure and the composition, it is investigated whether the semiconducting properties can be designed to attain, *e.g.*, promising thermoelectric materials. In the structures of many silicon-rich binary compounds with alkali- or alkaline earth metals, the electropositive metal atoms are encapsulated in large polyhedral cages formed by a typical four-bonded silicon framework. However, while an empty allotrope Si₄₆ would be a semiconductor, filled clathrates such as Ba_{8-x}Si₄₆ are metallic conductors.¹ Here the valence electrons of the electropositive elements are not necessary for building up the four-bonded silicon framework and the excess electrons occupy conduction bands instead.² To attain semiconducting behavior, the silicon atoms can be substituted by group 13 atoms like in the clathrate-I phase Rb₈Ga₈Si₃₈³ in which the four-bonded Ga atoms act as an electron sink. Another possibility is the substitution of silicon by transition metal atoms. In phases such as Ba₈Rh_{2.7}Si_{46-x-y},^{4,5} Ba₈Ni_xSi_{46-x-y}⁶⁻⁸ or Ba₈Au_xSi_{46-x}⁹⁻¹¹ the transition metal atoms are incorporated into the silicon framework. However, in this case, the understanding of the influence of the substituting elements on the physical properties is less straightforward. In compounds with higher content of

transition metals, structural motifs appear which differ from the clathrate networks. In this work, we introduce the semiconducting compound BaRh₂Si₉, representing a new type of crystal structure based on four-bonded silicon atoms with unexpected bond angles. This compound was originally found in the course of investigations on the phase relations in the system Ba/Rh/Si at 950 °C (τ_1 -Ba_{8.5}Rh_{17.5}Si₇₄ in ref. 5) and as a decomposition product of the clathrate-I phase Ba₈Rh_{2.7}Si_{42.6} at low temperatures.⁴

2. Methods

2.1 Synthesis

Starting materials for the preparation of BaRh₂Si₉ were BaSi, obtained by reaction of the elemental components in sealed tantalum containers under an Ar atmosphere, rhodium and silicon (Ba, ChemPur, 99.9%; Rh, Degussa, powder 99.9%; Si, ChemPur, 99.999%, finely ground in a boron carbide mortar). Mixtures of the components (up to 1 g) were pressed to pellets and arc melted several times under an Ar atmosphere (weight loss <0.5%). All operations were performed in an Ar filled glove box. The as cast alloys consisted of BaRh₂Si₉ as the main phase with varying amounts of Si, RhSi, BaSi₂, and the clathrate phase Ba₈Rh_{2.7}Si_{42.6}. Nearly single phase BaRh₂Si₉ was obtained by annealing the as cast buttons in glassy carbon crucibles enclosed in quartz glass ampoules under an Ar atmosphere at 950 °C for eight weeks. Alternatively, BaRh₂Si₉ can be synthesized in a solid state reaction from a compacted powder mixture of BaSi, Rh and Si by repeated annealing at 950 °C and regrinding.

^aMax Planck Institut für Chemische Physik fester Stoffe, Nöthnitzer Straße 40, 01187 Dresden, Germany

^bDepartment für Chemie, Institut für Anorganische Chemie, Universität zu Köln, Greinstraße 6, 50939 Köln, Germany. E-mail: grin@cpfs.mpg.de, jung@cpfs.mpg.de

2.2 X-Ray powder diffraction (XRPD)

Phase analysis on powder samples was performed with the X-ray Guinier diffraction technique (Huber G670 camera, Cu K α_1 radiation, $\lambda = 1.54056 \text{ \AA}$, germanium monochromator, $5^\circ \leq 2\theta \leq 100^\circ$, $\Delta 2\theta = 0.005^\circ$). The reflection positions were determined by profile deconvolution and the unit cell parameters were calculated from least-square refinement.¹²

2.3 X-Ray single crystal diffraction

Single crystals of BaRh₂Si₉ were selected under paraffin oil and fixed in a glass capillary (borosilicate glass, $\varnothing = 0.2 \text{ mm}$, wall thickness 0.01 mm, Hilgenberg). The measurements were performed using a CAD4 diffractometer (CAD4, Enraf-Nonius; graphite monochromator, MoK α radiation). Absorption corrections were performed using a ψ -scan procedure. The crystal structure was solved by direct methods with SHELXS¹³ and refined with WINCSD.¹² Details of the data collection and structure refinement are given in Table 1. Atomic parameters are listed in Table 2, and selected interatomic distances and angles in Tables 3 and 4, respectively.

2.4 Thermal analysis

For the measurement, 23 mg of substance were filled in a glassy carbon crucible ($\varnothing 4 \text{ mm}$, Sigradur G, HTW) and sealed in a Nb ampoule ($\varnothing 5 \text{ mm}$). A Netzsch heat-flux calorimeter DSC 404 C was used with a heating rate of 5 K min^{-1} and $T_{\text{max}} = 1473 \text{ K}$.

2.5 SEM

Samples were polished on air with discs of micrometer-sized diamond powders in paraffin and investigated using a Philips XL 30 scanning electron microscope (LaB₆ cathode). Energy dispersive X-ray spectroscopy (EDXS) was performed with an attached EDAX Si (Li) detector.

Table 1 Crystallographic data of BaRh₂Si₉

Refined composition	BaRh ₂ Si ₉
Crystal system	Monoclinic
Space group	C2/c
Lattice parameters (powder data)	$a = 6.2221(5) \text{ \AA}$ $b = 21.399(2) \text{ \AA}$ $c = 6.2272(5) \text{ \AA}$ $\beta = 90.306(7)^\circ$ $V = 829.1(2) \text{ \AA}^3$
Formula units/cell, Z	4
Calculated density	$4.774(1) \text{ g cm}^{-3}$
Absorption coefficient	9.8 mm^{-1}
Crystal size	$0.1 \times 0.05 \times 0.01 \text{ mm}^3$
Diffractometer	CAD4
Radiation	MoK α
θ_{max} for data collection	30°
Ranges for h, k, l	$-8/8, -5/30, -8/8$
Reflections measured	3043
Unique	1152
$I > 4\sigma(I)$	737
R_{int}	0.0526
R_σ	0.0590
Refined parameters	58
$R(F)$	0.0457

Table 2 Atomic coordinates and displacement parameters (in pm²) for BaRh₂Si₉^a

Atom	Site	x	y	z	Occ.	U_{eq}
Ba1	4e	0	0.68717(6)	1/4	1	124(4)
Rh1	4e	0	0.06959(7)	1/4	1	60(4)
Rh2	4e	0	0.43173(7)	1/4	1	69(4)
Si1	8f	-0.0004(6)	0.1603(2)	0.0241(6)	1	93(10)
Si2	8f	0.2266(6)	0.3410(2)	0.2534(6)	1	91(10)
Si3	8f	0.3714(6)	0.4556(2)	0.1100(6)	1	92(10)
Si4	8f	0.3721(6)	0.0445(2)	0.3889(6)	1	101(10)
Si5	4e	0	0.2505(3)	1/4	1	92(13)

Atom	U_{11}	U_{22}	U_{33}	U_{12}	U_{13}	U_{23}
Ba1	118(6)	146(6)	107(6)	0	9(4)	0
Rh1	69(6)	62(7)	49(6)	0	6(5)	0
Rh2	68(6)	69(6)	70(6)	0	6(5)	0
Si1	100(20)	80(20)	100(20)	10(14)	21(14)	-7(14)
Si2	70(20)	110(20)	100(20)	-6(14)	2(13)	5(14)
Si3	100(20)	100(20)	70(20)	18(14)	13(13)	4(13)
Si4	100(20)	100(20)	100(20)	-11(14)	0(13)	8(14)
Si5	90(20)	80(20)	100(20)	0	0(20)	0

^a U_{eq} is defined as one third of the trace of the orthogonalized U_{ij} tensor: $U_{\text{eq}} = 1/3[U_{22} + 1/\sin^2\beta(U_{11} + U_{33} + 2U_{13}\cos\beta)]$. The anisotropic displacement factor T is defined as $T = \exp[-2\pi^2(U_{11}a^2h^2 + \dots + 2U_{23}b^*c^*kl)]$.

Table 3 Selected interatomic distances (\AA)

Ba1	-2 Si4	3.272(4)	Si1	-1 Si2	2.387(5)
	-2 Si5	3.388(2)		-1 Si5	2.390(6)
	-2 Si5	3.394(3)		-1 Rh1	2.398(4)
	-2 Si1	3.458(4)		-1 Si2	2.434(5)
	-2 Si2	3.460(4)			
	-2 Si1	3.467(4)	Si2	-1 Si1	2.387(5)
Rh1	-2 Si2	3.485(4)		-1 Si5	2.396(6)
	-2 Si1	3.684(4)		-1 Rh2	2.399(4)
	-2 Si2	3.706(4)		-1 Si1	2.434(5)
	-2Rh1	4.002(1)			
	-2 Rh2	4.023(1)	Si3	-1 Si3	2.361(5)
				-1 Si4	2.433(5)
				-1 Rh1	2.446(4)
				-1 Rh2	2.527(4)
			Si4	-1 Si4	2.358(5)
				-1 Si3	2.433(5)
Rh2	-2 Si2	2.399(4)		-1 Rh2	2.435(4)
	-2 Si4	2.435(4)		-1 Rh1	2.525(4)
	-2 Si3	2.527(4)			
	-2 Si4	2.688(4)	Si5	-1 Si1	2.390(6)
			-1 Si1	2.390(6)	
			-1 Si2	2.396(6)	
			-1 Si2	2.396(6)	

2.6 Magnetic susceptibility

A polycrystalline sample of composition BaRh₂Si₉ ($m = 80 \text{ mg}$) was mounted in a polyethylene holder and measured in a SQUID magnetometer (MPMS-XL7, Quantum Design) in fields μ_0H from 2 mT to 7 T and in the temperature range 2–400 K. The diamagnetic contribution of the sample holder was subtracted.

2.7 Thermal and electric transport measurements

Thermopower, thermal and electrical conductivity measurements from 2 K to 350 K were simultaneously performed by a

Table 4 Selected interatomic angles at the Si atoms in the Rh–Si framework

Rh1–Si1–Si5	108.0(2)	Rh1–Si4–Si3	66.20(14)
Rh1–Si1–Si2	113.8(2)	Rh1–Si4–Si4	111.7(2)
Rh1–Si1–Si2	114.1(2)	Rh1–Si4–Rh2	124.5(2)
Si2–Si1–Si5	115.1(2)	Rh2–Si4–Si3	111.2(2)
Si2–Si1–Si5	115.4(2)	Rh2–Si4–Si4	117.4(2)
Si2–Si1–Si5	89.8(2)	Si3–Si4–Si4	115.1(2)
Rh2–Si2–Si1	114.6(2)	Si1–Si5–Si1	72.2(2)
Rh2–Si2–Si1	115.6(2)	Si1–Si5–Si2	130.5(2)
Rh2–Si2–Si5	107.9(2)	Si1–Si5–Si2	130.5(2)
Si1–Si2–Si1	90.2(2)	Si1–Si5–Si2	131.1(2)
Si1–Si2–Si5	113.5(2)	Si1–Si5–Si2	131.1(2)
Si1–Si2–Si5	114.4(2)	Si2–Si5–Si2	72.1(2)
Rh1–Si3–Si4	112.5(2)		
Rh1–Si3–Si3	117.0(2)		
Rh1–Si3–Rh2	125.2(2)		
Rh2–Si3–Si4	65.60(14)		
Rh2–Si3–Si3	113.3(2)		
Si3–Si3–Si4	114.7(2)		

relaxation method and ac resistance measurements, respectively, using a commercial measurement system (PPMS, Quantum Design). The thermal and electrical contacts were glued to the sample with a silver filled conductive epoxy adhesive.

2.8 Quantum-chemical calculation procedures

Electronic structure calculations were performed by using the all-electron, full-potential local orbital (FPLO) method¹⁴ within the local density approximation to the density functional theory. Perdew–Wang parameterization for the exchange–correlation potential was employed.¹⁵ The electron localizability indicator in the ELI-D representation¹⁶ was calculated with the module implemented in the program package FPLO.¹⁷ Topological analysis of the electron density and the ELI-D was carried out by using the program DGRID.¹⁸ A combined analysis of the electron density and ELI-D was performed using the basin intersection technique.¹⁹ The atomic charges are calculated using the quantum theory of atoms in molecules (QTAIM) approach.²⁰

3. Results and discussion

3.1 Phase relations

Three ternary compounds have been known in the system Ba–Rh–Si, namely BaRh₂Si₂,²¹ BaRh₃Si₂,²² and the clathrate-I phase Ba₈Rh_xSi_{46–x–y} (2.4 < x < 2.7; y = 0.7 for x = 2.7).⁴ The new compound BaRh₂Si₉ was first identified by annealing of the high-temperature phase Ba₈Rh_xSi_{46–x–y} at 840 °C, where the clathrate phase decomposed into BaRh₂Si₉, BaSi₂ and Si.

At the nominal composition BaRh₂Si₉, the relative amounts of phases formed on cooling from the melt depend strongly on the cooling rate. In a sample prepared in a glassy carbon crucible in a high frequency furnace and cooled from the melt to about 800 °C within three minutes and then to room temperature outside the furnace, the components found by means of

XRPD were the clathrate-I phase, Si, RhSi, and BaSi₂, but no BaRh₂Si₉. In contrast, on rapid cooling of arc-melted samples with the same nominal composition on a water-cooled copper hearth, the formation of the clathrate-phase is suppressed to a large extent. Instead, BaRh₂Si₉ is obtained as the main phase with additional by-products Si, Rh₃Si₄, BaSi₂, and, in a small amount, clathrate-I.

The thermal stability of BaRh₂Si₉ was investigated by DSC and annealing experiments. After annealing experiments at 970 °C, no decomposition was observed. After 12 h at 1000 °C and cooling within a few minutes, the sample consisted of BaRh₂Si₉, clathrate phase, Si, Rh₃Si₄, and BaSi₂ indicating decomposition of the compound. This is in agreement with a DSC experiment which showed on heating one pronounced endothermic effect at 980 °C.

3.2 Crystal structure

The structure of BaRh₂Si₉ was solved in the centrosymmetric monoclinic space group *C2/c*. The lattice parameters (Table 1) are close to an orthogonal unit cell and in fact the arrangement of most of the atoms (Ba1, Rh1, Rh2, Si1, Si2, Si5) can nearly be described in the orthorhombic space group *Cmcm*. However, the silicon sites Si3 and Si4 clearly break the orthorhombic symmetry. All crystallographic sites were found to be fully occupied, which is in agreement with the EDXS analysis. The displacement parameters *U*_{ij} were widely isotropic. The crystal structure of BaRh₂Si₉ is characterized by a 3D Si–Rh framework in which the Rh atoms are located within adjacent layers extending perpendicular to the *b* axis shortly below and above *y* = 0 and *y* = 1/2 (Fig. 1a). The rhodium atoms are coordinated by 6 silicon atoms forming heavily distorted trigonal prisms, which are corner-connected (Fig. 2). Between the two double layers [RhSi₆], large polyhedral cavities accommodate the Ba atoms. The polyhedra around the Ba atoms, marked in blue in Fig. 1b and shown separately in Fig. 3a, are also arranged in double layers and consist of 18 Si atoms (Si1, Si2,

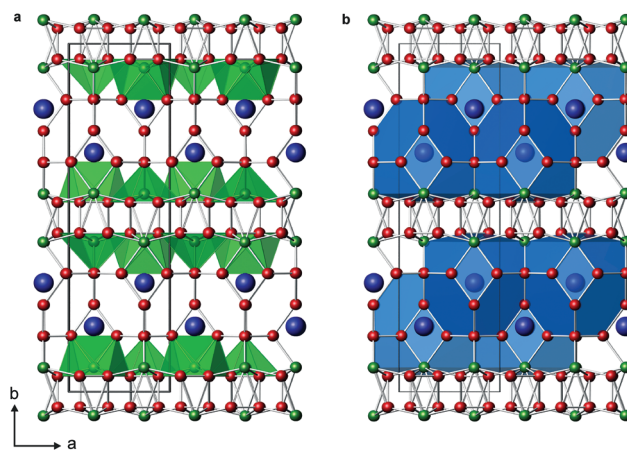


Fig. 1 Crystal structure of BaRh₂Si₉ in projection along [001]. Ba atoms are drawn in blue, Rh atoms in green and silicon atoms in red. (a) The distorted [RhSi₆]-prisms are highlighted in green, (b) the double-layers of BaSi₁₈Rh₄ polyhedra are highlighted in blue.

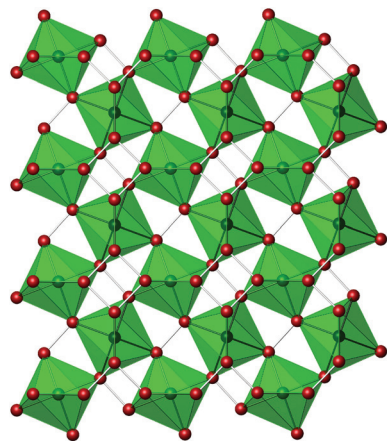


Fig. 2 Layer of distorted $[\text{RhSi}_6]$ -polyhedra perpendicular to $[010]$.

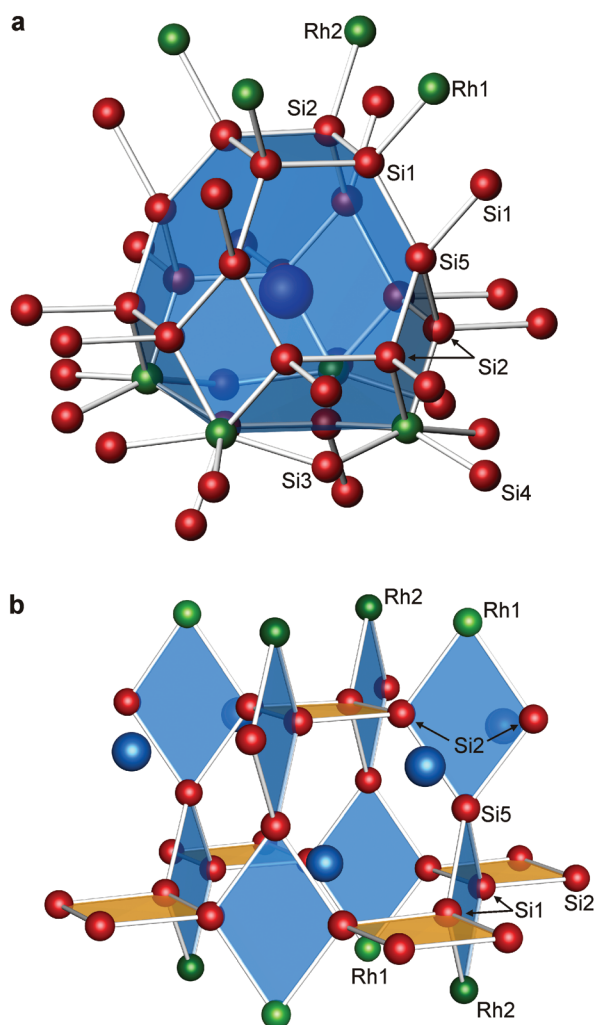


Fig. 3 (a) Local atomic arrangement around a polyhedron $\text{BaSi}_{18}\text{Rh}_4$. (b) Building elements with unusually small bond angles highlighted.

Si_4 , Si_5 ; $d(\text{Ba}-\text{Si}) = 3.272(4) \text{ \AA} - 3.706(4) \text{ \AA}$ and four Rh atoms ($d(\text{Ba}-\text{Rh}) = 4.002(1) - 4.023(1) \text{ \AA}$). The Si_3 atoms with a distance of $4.435(4) \text{ \AA}$ to the Ba atoms are not considered as part of the

coordination sphere. The upper part of the $\text{BaSi}_{18}\text{Rh}_4$ polyhedron with a slightly distorted square (Si_4) at the top, four adjacent hexagonal faces (Si_6), and four lateral rhombic faces (Si_3Rh) is closely related to a truncated octahedron, known f.e. from the structure of sodalite. Deviating from a truncated octahedron, the bottom of the polyhedron is formed by each of the two bent hexagonal (Si_4Rh_2) and pentagonal faces (Si_3Rh_2). Every polyhedron is face-connected to 8 others. Four of them, connected by rhombic faces, are in the same orientation, while those sharing hexagonal faces are in reverse orientation (Fig. 1b). All the Si atoms are connected to 4 nearest neighbors. These are four silicon atoms in the case of Si_5 , three silicon atoms and one rhodium atom for Si_1 and Si_2 , and two silicon and two rhodium atoms for Si_3 and Si_4 . The distances roughly correspond to the sum of the covalent radii $r_{\text{Si}} = 1.17 \text{ \AA}$ and $r_{\text{Rh}} = 1.25 \text{ \AA}$:²³ $d(\text{Si}-\text{Si}) = 2.358(5) - 2.434(5) \text{ \AA}$, $d(\text{Si}-\text{Rh}) = 2.398(4) - 2.527(4) \text{ \AA}$. While bonding angles in four-connected silicon frameworks are usually close to the tetrahedral angle of 109.5° , the respective angles in BaRh_2Si_9 are most remarkable. For Si_1 and Si_2 , which constitute the square at the top of the BaRh_2Si_9 polyhedron (Fig. 3a) the angles $\text{Si}_2-\text{Si}_1-\text{Si}_2$ and $\text{Si}_1-\text{Si}_2-\text{Si}_1$ are close to 90° . Even smaller angles are observed for

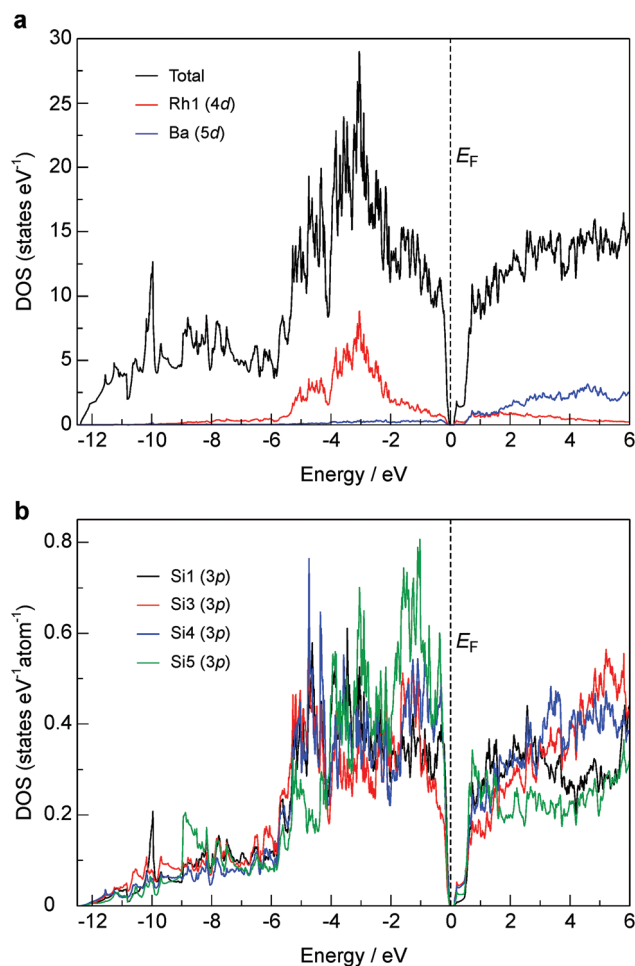


Fig. 4 (a) Total electronic density of states together with Rh and Ba d-state contributions. (b) Partial density of states due to Si 3p-state contributions.

the Si5 atoms, which, together with Si1, Si2 and a rhodium atom constitute the lateral rhombic faces of the polyhedra. The bond angles Si1–Si5–Si1 and Si2–Si5–Si2 were determined to be only $\approx 72^\circ$. The arrangement of these unusual building elements is shown in Fig. 3b.

3.3 Electronic structure and chemical bonding

Band structure calculations were performed using the experimentally determined structural data. BaRh_2Si_9 is found to be semiconducting with a band gap of 0.12 eV. The total density of states (DOS) and some selected partial DOS are shown in Fig. 4. The Rh1 and Rh2 atoms as well as the Si1 and Si2 atoms have very similar partial DOS; therefore only Rh1 and Si1 contributions are presented. States between ≈ -12.5 eV and -7 eV are dominated by Si 3s states, while the hybridization of Rh 4d and Si 3p states is more pronounced between -5 and -1 eV. Population analysis based on the projected DOS reveals that Ba 5d states are occupied by 0.65 electron and the Rh 4d basis functions by 8.0 electrons. A more accurate and basis set independent method to obtain the effective charge of atoms is the QTAIM approach. Here we find that the Rh atoms gain one electron extra while the Ba atoms lose 1.3 electrons. The silicon atoms in BaRh_2Si_9 show a non-uniform charge distribution. The Si5 atoms with only Si near neighbors are negatively charged by 0.6 excess electron, while Si1 and Si2 with

one Rh neighbor are positively charged by 0.1 electron, and Si3 and Si4 with two Rh neighbors by 0.2 electron. Taking into account the site multiplicities, these results suggest in total a balance of $[\text{Ba}^{1.3+}][\text{Rh}_2\text{Si}_9]^{1.3-}$.

The analysis of the ELI yields predominantly two-center Si–Si and Si–Rh bonds (Fig. 5). The Si5–Si1, Si5–Si2 and Si1–Si2 bonds have two electrons in their basins, but the electron counts of the bonds involving Si3 and Si4 atoms are each higher than two: $2.3 e^-$ for Si3–Si3, $2.5 e^-$ for Si4–Si4 and $2.2 e^-$ for Si3–Si4. This latter group of bonds can be described by quasi-two-center bonds with additional Rh atom contributions of approximately 0.2 electron in each case: Rh2 contributes to the Si3–Si3, Rh1 to the Si4–Si4, and both Rh1 and Rh2 to the Si3–Si4 interaction. The Si1–Rh and Si2–Rh bond basins each have 1.7 electrons. The Si3–Rh1 (Si4–Rh1) and Si3–Rh2 (Si4–Rh2) bond basins contain 0.8 (1.7) and 1.6 (1.0) electrons, respectively, emphasizing the slightly different bonding behaviors of the Si3 and Si4 atoms. In Si–Rh bonds, the Rh atoms contribute around 35% of the total electron counts implying moderately polar covalent bonds. For comparison, in the clathrate I phase with an Rh–Si framework, $\text{Ba}_8\text{Rh}_x\text{Si}_{46-x-y}\square_y$, the Rh atoms contribute to the Si–Rh bonds by 40%.⁴ Although the Rh atoms are 4-coordinated with Si in the clathrate but 6-coordinated in BaRh_2Si_9 , the number of electrons in Rh atom basins is essentially the same. Fig. 5c

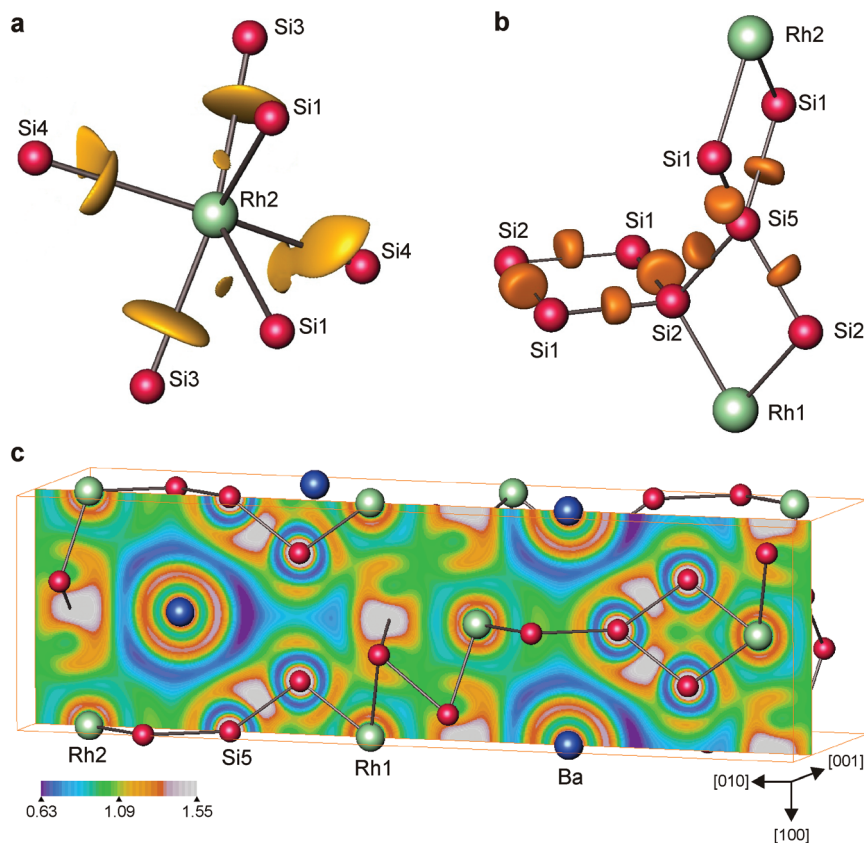


Fig. 5 (a) ELI-D with an isosurface value of $\nu = 1.271$ in the first coordination shell of the Rh2 atoms. (b) ELI-D with an isosurface value of $\nu = 1.515$ in the Si₄ and Si₃Rh rings revealing the covalent Si–Si and Si–Rh interactions. (c) ELI-D distribution in a plane perpendicular to [001] ($z = 0.25$) showing the structuring of the penultimate shells of Ba and Rh atoms and direct Rh–Si interactions.

shows the structuring of the ELI distribution in the penultimate shells of Ba ($n = 5$) and Rh ($n = 4$) atoms. The observed deviation from the spherical distribution, which would be expected for chemically inert core shells, indicates that electrons belonging to these shells (mainly Ba 5d and Rh 4d) participate in chemical bonding. Apart from this, Ba atom interactions with the Si–Rh substructure are mostly of ionic character.

3.4 Physical properties

BaRh₂Si₉ shows a negative, weakly temperature-dependent magnetic susceptibility which is well described by $\chi(T) = \chi_0 + C/T$. Here, χ_0 is the diamagnetic temperature-independent intrinsic susceptibility of the compound and C/T is a paramagnetic Curie term due to impurities and charged defects. A fit results in $\chi_0 = -210(10) \times 10^{-6} \text{ emu mol}^{-1}$ and $C = 8 \times 10^{-5} \text{ emu K mol}^{-1}$; the latter would correspond to a concentration of hypothetical $S = 1/2$ impurities of 0.02%. The diamagnetism of BaRh₂Si₉ is stronger than the sum of the closed-shell diamagnetic increments which is calculated to be $\chi_{\text{dia}} \approx -126 \times 10^{-6} \text{ emu mol}^{-1}$ (Ba²⁺: $-32 \times 10^{-6} \text{ emu mol}^{-1}$,²⁴ Rh⁴⁺: $-18 \times 10^{-6} \text{ emu mol}^{-1}$,²⁵ and α -Si: $-6.4 \times 10^{-6} \text{ emu mol}^{-1}$, ref. 26). The electrical conductivity (Fig. 6a) of BaRh₂Si₉ is of the thermally-activated type with resistivity values of 0.5 m Ω m at 300 K, 2.7 m Ω m at 77 K, and 15 m Ω m at 4.2 K. The Seebeck coefficient (Fig. 6b) is positive and increases with temperature, running through a broad maximum of +215 $\mu\text{V K}^{-1}$ at $T \approx 250$ K. The thermal conductivity $\kappa(T)$ (Fig. 6c) increases first rapidly with increasing temperature. In this low-temperature region it can be described with a power law $\kappa(T) \propto T^\alpha$ with $\alpha \approx 2.4$. Then, $\kappa(T)$ shows a pronounced maximum of 27 $\text{W m}^{-1} \text{K}^{-1}$ at $T \approx 40$ K followed by a decrease with $\kappa(T) \propto T^{-1}$. Such a temperature dependence of the thermal conductivity with a Debye-law region at low temperatures, a typical phonon peak and a decrease proportional to $1/T$ is characteristic of a well-crystallized material without free charge carriers. The observed transport properties thus indicate that BaRh₂Si₉ is a p-type semiconductor. The regime of intrinsic conduction is expected for temperatures above those of the present resistivity data. An estimate of the doping level energy from the data between 330 K and 350 K gives ≈ 0.06 eV.

5. Conclusion

BaRh₂Si₉ is a new type of clathrate-like cage structure in which Ba atoms are encapsulated in an Rh–Si-framework. The framework comprises structure elements with unusually small Si–Si–Si bond angles. According to quantum chemical calculations, BaRh₂Si₉ is electronically balanced. The Ba atoms and the Si atoms adjacent to Rh are positively charged, while the Rh atoms and the remaining Si atoms are negatively charged. Thermoelectric transport measurements indicate that BaRh₂Si₉ is a p-type semiconductor, in agreement with the observed diamagnetism and with band structure calculations.

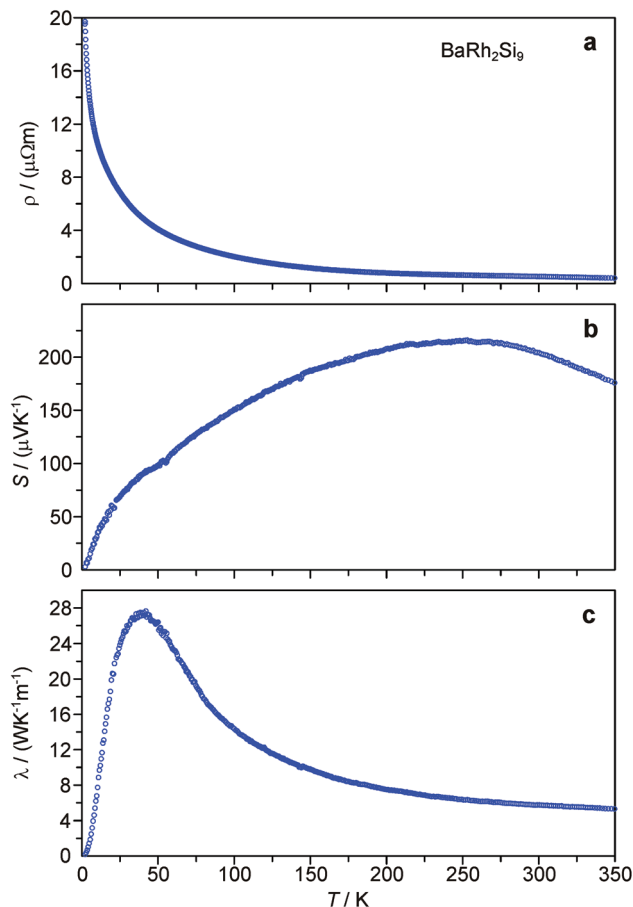


Fig. 6 Temperature dependence of the transport properties of BaRh₂Si₉: (a) electrical resistivity showing semiconducting behavior; (b) thermopower indicating p-type conduction, and (c) thermal conductivity typical of a well-crystallized semiconducting material.

Acknowledgements

The authors thank the competence groups *Metallography* and *Structure* at MPI CPFS. M. B., H. D. N., and Yu. G. gratefully acknowledge financial support from the Deutsche Forschungsgemeinschaft (SPP 1415). A. O. thanks Ulrike Nitzsche (IFW Dresden) for help in computational aspects.

References

- 1 S. Yamanaka, *Dalton Trans.*, 2010, **39**, 1901–1915.
- 2 C. Cros, M. Pouchard and P. Hagenmuller, *J. Solid State Chem.*, 1970, **2**, 570–581.
- 3 H. G. von Schnering, R. Kröner, H. Menke and K. Peters, *Z. Kristallogr. – New Cryst. Struct.*, 1998, **213**, 677–678.
- 4 W. Jung, H. Kessens, A. Ormeci, W. Schnelle, U. Burkhardt, H. Borrmann, H. D. Nguyen, M. Baitinger and Y. Grin, *Dalton Trans.*, 2012, **41**, 13960–13968.
- 5 M. Falmbigl, A. Grytsiv, P. Rogl and G. Giester, *Intermetallics*, 2013, **36**, 61–72.

- 6 J. H. Roudebush, M. Orellana, S. Bux, T. Yi and S. M. Kauzlarich, *J. Solid State Chem.*, 2012, **192**, 102–108.
- 7 M. Falmbigl, M. X. Chen, A. Grytsiv, P. Rogl, E. Royanian, H. Michor, E. Bauer, R. Podloucky and G. Giester, *Dalton Trans.*, 2012, **41**, 8839–8849.
- 8 U. Aydemir, C. Candolfi, A. Ormeci, H. Borrmann, U. Burkhardt, Y. Oztan, N. Oeschler, M. Baitinger, F. Steglich and Yu. Grin, *Inorg. Chem.*, 2012, **51**, 4730–4741.
- 9 G. Cordier and P. Woll, *J. Less-Common Met.*, 1991, **169**, 291–302.
- 10 N. Jaussaud, P. Gravereau, S. Pechev, B. Chevalier, M. Ménétrier, P. Dordor, R. Decourt, G. Goglio, C. Cros and M. Pouchard, *C. R. Chim.*, 2005, **8**, 39–46.
- 11 C. Candolfi, U. Aydemir, M. Baitinger, N. Oeschler, F. Steglich and Yu. Grin, *J. Appl. Phys.*, 2012, **111**, 043706.
- 12 L. G. Akselrud, P. Y. Zavali, Yu. Grin, V. K. Pecharsky, B. Baumgartner and E. Wölfel, *Mater. Sci. Forum*, 1993, **133–136**, 335–340.
- 13 G. M. Sheldrick, *SHELXS-97*, Göttingen, 1997.
- 14 K. Koepf and H. Eschrig, *Phys. Rev. B: Condens. Matter*, 1999, **59**, 1743–1757.
- 15 J. P. Perdew and Y. Wang, *Phys. Rev. B: Condens. Matter*, 1992, **45**, 13244–13249.
- 16 M. Kohout, *Int. J. Quantum Chem.*, 2004, **97**, 651–658.
- 17 A. Ormeci, H. Rosner, F. R. Wagner, M. Kohout and Yu. Grin, *J. Phys. Chem. A*, 2006, **110**, 1100–1105.
- 18 M. Kohout, *Program DGRID, version 4.6*, 2011.
- 19 S. Raub and G. Jansen, *Theor. Chem. Acc.*, 2001, **106**, 223–232.
- 20 R. F. W. Bader, *Atoms in Molecules, A Quantum Theory*, Clarendon Press, Oxford, 1995.
- 21 D. Langen, S. Schoolaert, H. Ploss and W. Jung, *Z. Anorg. Allg. Chem.*, 1997, **623**, 1561–1566.
- 22 H. Ploss, Dissertation, Universität zu Köln, 1998.
- 23 J. Emsley, *The elements, de Gruyter*, Berlin, New York, 1994.
- 24 E. S. R. Gopal, *Specific Heat at Low Temperatures*, Plenum Press, London, 1966.
- 25 P. W. Selwood, *Magnetochemistry*, Interscience, New York, 2nd edn, 1956.
- 26 S. Hudgens, M. Kastner and H. Fritzsche, *Phys. Rev. Lett.*, 1974, **33**, 1552–1555.